

# Structural Characterization of $\text{Al}_x\text{Ga}_{1-x}\text{Sb}$

JOEL DÍAZ-REYES

Centro de Investigación en Biotecnología Aplicada  
Instituto Politécnico Nacional

. Ex-Hacienda de San Molino. Km 1.5 de la Carretera Estatal Santa Inés Tecuexcomac-Tepetitla.  
Tepetitla, Tlaxcala. 90700.

MEXICO

joel\_diaz\_reyes@hotmail.com <http://www.cibatlaxcala.ipn.mx>

JOSÉ ELADIO FLORES-MENA

Facultad of Ciencias de la Electrónica

Benemérita Universidad Autónoma de Puebla

Av. San Claudio y 18 Sur, Ciudad Universitaria, Puebla, Puebla. 72570.

MEXICO

JOSÉ MOISÉS GUTIÉRREZ-ARIAS

Facultad of Ciencias de la Electrónica

Benemérita Universidad Autónoma de Puebla

Av. San Claudio y 18 Sur, Ciudad Universitaria, Puebla, Puebla. 72570

MEXICO

MARÍA MONTSERRAT MORIN-CASTILLO

Facultad of Ciencias de la Electrónica

Benemérita Universidad Autónoma de Puebla

Av. San Claudio y 18 Sur, Ciudad Universitaria, Puebla, Puebla. 72570.

MEXICO

**Abstract:** - Using the liquid phase epitaxy technique under supercooling conditions we have grown  $\text{Al}_x\text{Ga}_{1-x}\text{Sb}$  layers doped with tellurium lattice-matched to (100) n-GaSb.  $\text{Al}_x\text{Ga}_{1-x}\text{Sb}$  ternary solid solutions with  $0.05 \leq x \leq 0.2$  were grown at 400°C. High resolution X-ray diffraction and Raman spectroscopy were used to characterize the structural quality of the grown  $\text{Al}_x\text{Ga}_{1-x}\text{Sb}$  layers. The out of plane lattice parameter was estimated directly from the asymmetrical diffractions (115) and (-1-15) alloy. These results show that some of the layers are more strained than others. The out of plane lattice parameter as a function of Al content is higher than the corresponding bulk lattice parameter of  $\text{Al}_x\text{Ga}_{1-x}\text{Sb}$  layers obtained with Vegard's law. Two peaks are observed in their Raman spectra over this composition range. The assignment of the observed vibrational modes to GaSb-like is discussed.

**Key-Words:** - Liquid phase epitaxy (LPE), III-V alloy compound semiconductors, AlGaSb, High resolution X-ray diffraction (HRXRD), Phonons, RAMAN spectroscopy

## 1 Introduction

Some years ago the research of several III-V semiconductor alloys is associated with the wavelength of the optical fiber loss minima (0.8  $\mu\text{m}$ ). In particular, gallium antimonide (GaSb) is interesting as a potential substrate material for devices in the band-gap range of 0.3-1.58 eV [1,2] and its related compounds are of interest as low band gap materials with applications in devices

operating in the infrared range. For this reason, it is necessary to improve the quality of GaSb and its alloys and to get a deep knowledge of their physical properties [3,4].

High resolution X-Ray diffraction (HRXRD) is applied in the investigation of epitaxial structures of semiconductors [5]. The lattice parameters of semiconductor alloys gradually change with the chemical composition giving rise to an increase of

strain until mismatch dislocations appear lead to the relaxation of the thin film.

Raman scattering is well known as a useful means of investigating the structures in semiconductors. Raman scattering (RS) can give effective information about various crystalline structures from single crystalline to amorphous samples. A number of Raman studies on single crystalline GaSb samples [6–8] and amorphous GaSb samples [9–11] have been reported.

In this work we present the study of the  $\text{Al}_x\text{Ga}_{1-x}\text{Sb}$  thin films for different Al molar concentrations. The samples were grown by liquid phase epitaxy (LPE) technique at  $400^\circ\text{C}$ . The structural characterization was made by HRXRD and Raman spectroscopy.

## 2 Experimental Details

Please, leave two blank lines between successive sections as here.  $\text{Al}_x\text{Ga}_{1-x}\text{Sb}$  ternary solid solutions with  $0.05 \leq x \leq 0.2$  were grown by liquid phase epitaxy on (001) oriented GaSb substrates. The  $\text{Al}_x\text{Ga}_{1-x}\text{Sb}/\text{GaSb}$  heterostructure studied in this work was grown by LPE at  $400^\circ\text{C}$ , using a sliding boat system under hydrogen stream in horizontal furnace and in its variant of super cooling technique [12]. We used n-type (100) GaSb substrates doped with Tellurium and with a free carrier concentration about  $\sim 4 \times 10^{17} \text{ cm}^{-3}$  at 300 K. Structural characterization of the samples was carried out by means of X-ray diffraction (XRD) in a Bruker D8 Discover diffractometer, parallel beam geometry and monochromator of gobe mirror,  $\text{CuK}\alpha$  radiation =  $1.5406 \text{ \AA}$ , in the range of  $20^\circ < 2\theta < 80^\circ$ , by step of  $0.02^\circ$ . The XRD data were refinement using the programs POWDERX and DICVOL04 to determine the crystal system, the parameters of unit cell, parallel ( $a_{\parallel}$ ) and perpendicular ( $a_{\perp}$ ) and the atomic fraction  $x$  corresponding. Raman scattering experiments were performed at room temperature using the  $6328 \text{ \AA}$  line of an Ar-ion laser at normal incidence for excitation. The light was introduced into a microscope having a  $50\times$  (numerical aperture 0.9) microscope objective. The measurements were made with a laser power of 20 mW. Care was taken not to heat the sample inadvertently to the point of changing its Raman spectrum. Scattered light was analysed using a Jobin-Yvon T64000 triple spectrometer, operating in the subtractive configuration, and a multichannel charge-coupled device (CCD) detector cooled to 140 K using liquid  $\text{N}_2$ . The CCD device was operated at low temperature to reduce the dark current caused by thermal electrons to obtain better signal-to-noise.

The typical aspect rum acquisition time was limited to 60 s to minimize the sample heating effects discussed above. Absolute spectral feature position calibration to better than  $0.5 \text{ cm}^{-1}$  was performed using the observed position of Si which is shifted by  $521.2 \text{ cm}^{-1}$  from the excitation line.

## 3 Results and Discussions

The  $\text{Al}_x\text{Ga}_{1-x}\text{Sb}$  surface morphology was generally very smooth with a root-mean-square (rms) roughness of 19–39  $\text{\AA}$  as was determined from tapping mode AFM. Images of two representative samples are shown in Figure 1. The surface shown in Figure 1a is rough (39  $\text{\AA}$  rms) while that in Figure 1b indicates the presence of some small hillocks. In order to determine the lattice parameter and the strain of the thin films, the rocking curves were obtained from the HRXRD measurements of  $\text{Al}_x\text{Ga}_{1-x}\text{Sb}$  films on GaSb substrates; the diffraction peaks of the alloys are as narrow as the substrate peak, indicative of good crystalline and homogenous composition of the layer [13]. It is known that the crystalline quality of semiconductor compounds obtained by the LPE technique is dependent on the growth temperature; at  $400^\circ\text{C}$  the films had good crystalline quality.

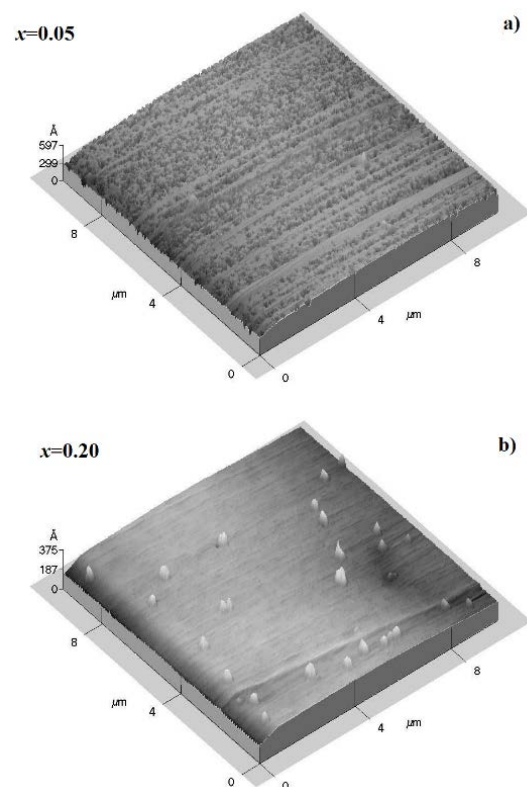


Figure 1. Atomic force microscopy images of  $\text{Al}_x\text{Ga}_{1-x}\text{Sb}$  layers grown on (100) GaSb: (a)  $x\sim 0.05$  with an rms roughness of 39 Å and (b)  $x\sim 0.20$  with rms roughness of 19 Å

Figure 2 shows the  $\text{AlGaSb}$  diffraction peak of the (004) plane is clearly separated from the (004) GaSb diffraction peak. The samples with an aluminium fraction 5, 10, 15 and 20 percent are presented in Figures 2a-d, respectively. As it is observed of this figure, the alloy diffraction peaks are as narrow as the substrate peak, indicative a good crystalline quality and homogeneous composition of the layer [13].

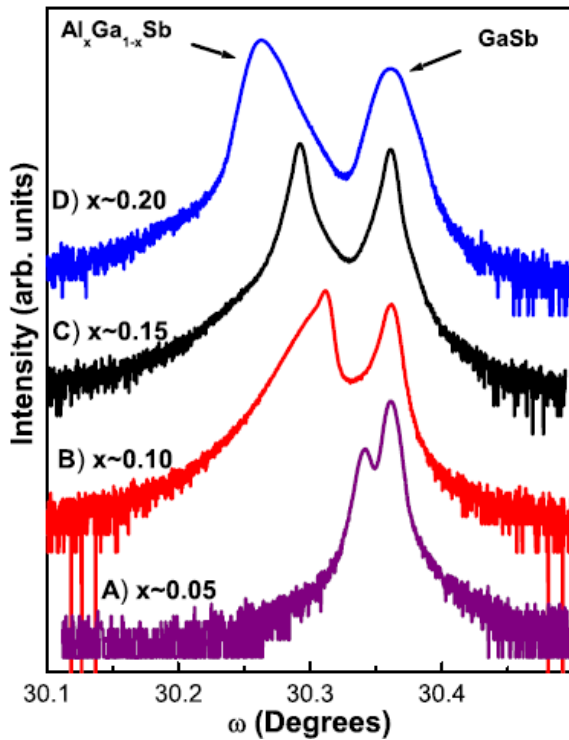


Figure 2. Experimental X-ray rocking curves of  $\text{Al}_x\text{Ga}_{1-x}\text{Sb}$  and GaSb from (004) reflection.

Figure 3a shows the  $\text{Al}_x\text{Ga}_{1-x}\text{Sb}$  diffraction peak of the symmetrical reflection (115) plane that is clearly separated from the (115) GaSb diffraction peak, the same occurs for asymmetrical reflection that is shown in Figure 3b. In order to determinate the alloy bulk lattice constant, it is necessary to know  $a_{\perp}$  and  $a_{\parallel}$ , these values were obtained using different reflections, [(115) and (-1-15)] and the Macrander's formulas [5]:

$$a_{\perp} = a_s \frac{\sin\theta_B}{\sin(\theta_B + \Delta\theta)} \frac{\cos\tau_S}{\cos(\tau_S + \Delta\tau)} \quad (1)$$

$$a_{\parallel} = a_s \frac{\sin\theta_B}{\sin(\theta_B + \Delta\theta)} \frac{\sin\tau_S}{\sin(\tau_S + \Delta\tau)} \quad (2)$$

where  $a_s$  is the substrate lattice constant,  $\theta_B$  is Bragg angle for (115) direction,  $\tau_S$  is the angle between (115) plane and the surface plane of the sample,  $\Delta\theta$  and  $\Delta\tau$ , which are obtained with the following equations [5]:

$$\Delta\theta = \frac{\Delta\omega^+ + \Delta\omega^-}{2} \quad (3)$$

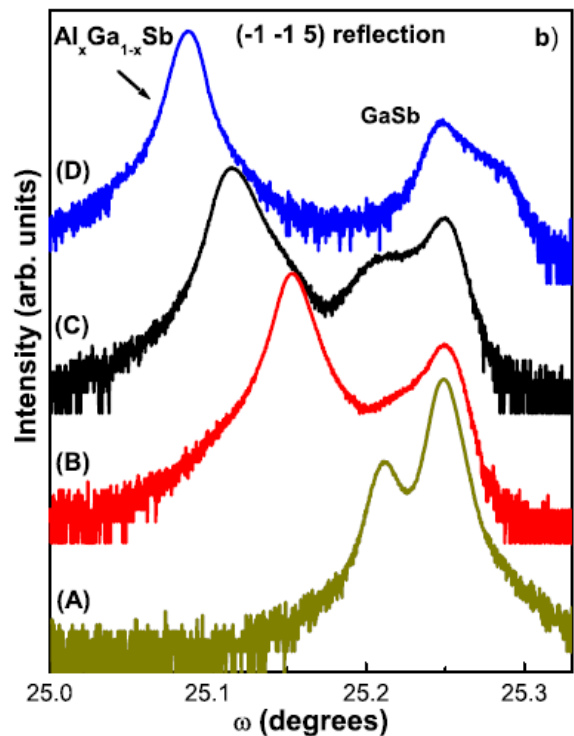
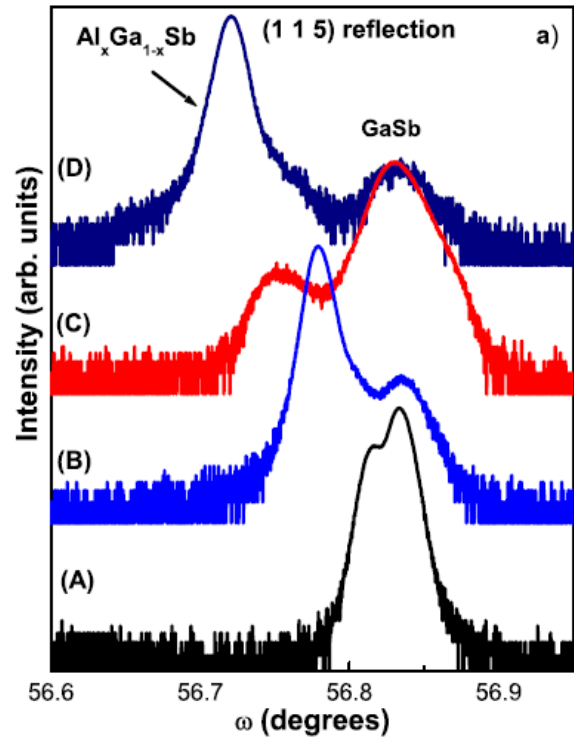


Figure 3. Experimental X-ray rocking curves of  $\text{Al}_x\text{Ga}_{1-x}\text{Sb}$  and GaSb from symmetrical and asymmetrical reflections: a) (115) plane and b) (-1-15) plane.

$$\Delta\tau = \frac{\Delta\omega^+ - \Delta\omega^-}{2} \quad (4)$$

$\Delta\omega^+$  is the difference between the peak and the layer peaks in (-1-15) direction,  $\Delta\omega^-$  is the difference between substrate and the layer peaks in (115) direction. It has found that the bulk lattice constant of the alloy  $a_o$  is related with orthogonal and parallel lattice constant of the grown films [14]. Thus can be deduced as:

$$a_o = a_{\parallel} + \frac{1-\nu(x)}{1+\nu(x)}(a_{\perp} - a_{\parallel}) \quad (5)$$

where  $\nu(x)$  is Poisson's ration. Table 1 shows lattice constants obtained from equations (1) to (4), and the aluminium fraction molar.

Table 1. Result of the analysis by HRXRD of the samples.

Sample	$a_{\perp}(\text{Å})$	$a_{\parallel}(\text{Å})$	$a_o(\text{Å})$	$x$
A	6.0994	6.0950	6.0973	0.0346
B	6.1055	6.0967	6.1012	0.1354
C	6.1097	6.0984	6.1042	0.2958
D	6.1134	6.1037	6.1087	0.3235

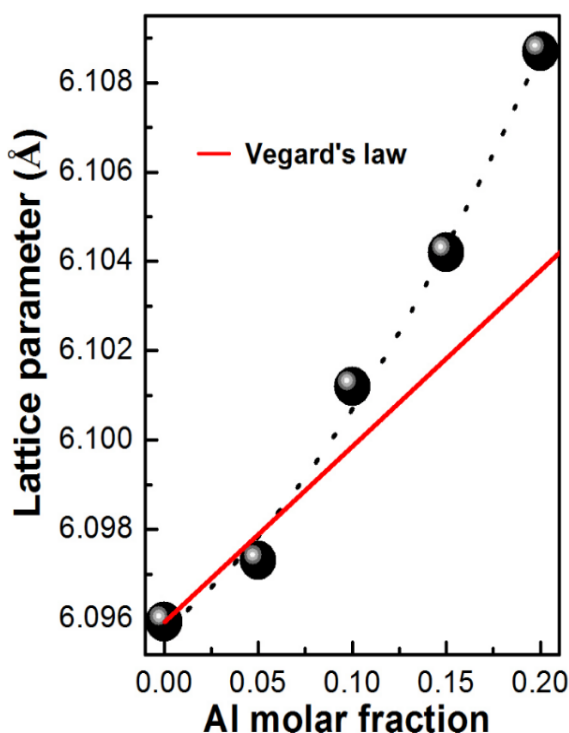


Figure 4.  $\text{Al}_x\text{Ga}_{1-x}\text{Sb}$  lattice parameter versus content of the layer. (—) Linear behaviour as expected from Vegard's law. The experimental values ( $\blacklozenge$ ) of the unstrained lattice constant can be described with a second-order polynomial (---).

In Figure 4 illustrates the values of the unstrained lattice constant of the epilayers that have been plotted versus an average Al composition. The lattice parameter values  $a_{\text{GaSb}}= 6.09593 \text{ Å}$  [15] and  $a_{\text{AlSb}}=6.1353 \text{ Å}$  [16] have been used as the extremes of the alloy range. The solid line represents the linear behaviour as expected from Vegard's law. The experimental values of the unstrained lattice constant can be described with a second-order polynomial shown in Figure 4 as the solid line fitting the experimental points:

$$a_o(x) = 6.09593 + 0.03425x + 0.1531x^2 \quad (6)$$

The Raman spectra for  $\text{Al}_x\text{Ga}_{1-x}\text{Sb}$  ternary alloys with different Al concentration are shown in Figure 5. The spectra show two peaks TO and LO over the entire composition range. The peak at approximately  $233 \text{ cm}^{-1}$  (wavenumber for the LO phonon in binary GaSb) [17] is assigned as the GaSb-like LO mode, see Figure 6. The TO mode is forbidden in the scattering configuration used, but it is seen as a shoulder or a tiny peak below the LO peak. The AlGaSb alloys show a two-mode behaviour. The mass of Ga (69.7 u) is larger than the reduced mass of AlSb (22.1 u). The mass of Al (27 u) is smaller than the reduced mass of GaSb (44.3 u). According to the mass criteria proposed by Chang and Miltra [18].

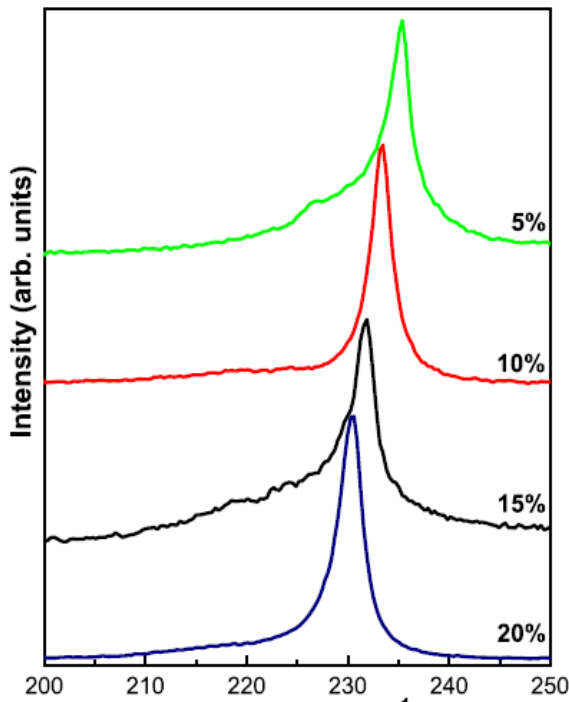


Figure 5. Room-temperature Raman spectra for  $Al_xGa_{1-x}Sb$  alloy over the frequency shift range.

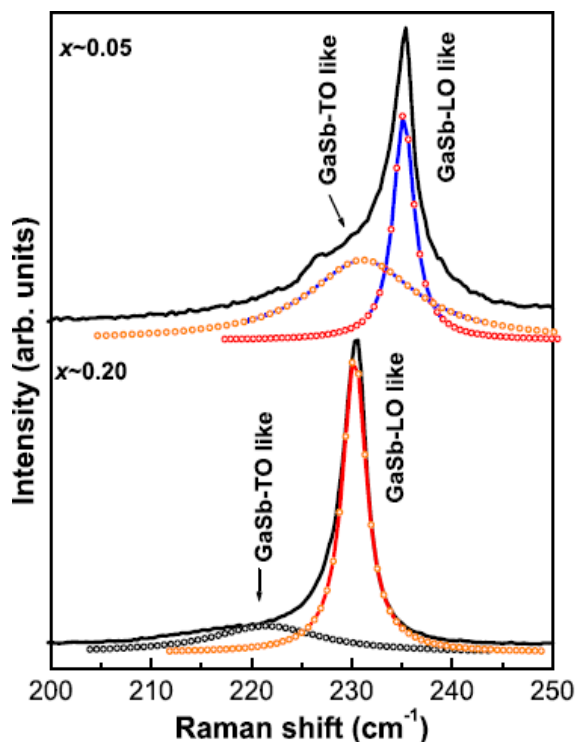


Figure 6. First-order Raman spectra of  $Al_xGa_{1-x}Sb$  at room temperature. Decomposition of the measured Raman spectra into individual components (Lorentzian shape) for two Al concentrations: (a)

5% and (b) 20% grown on n-type substrates. The dashed lines are their respective fitting.

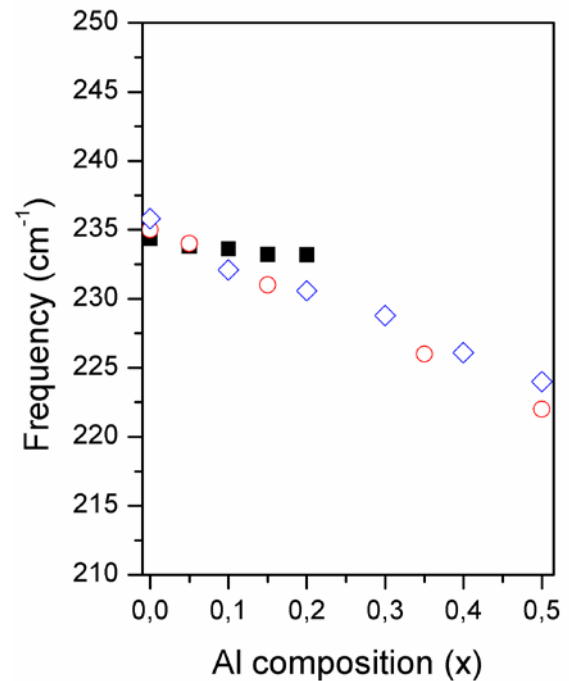


Figure 7. Compositional dependence of GaSb-like LO phonons. (■) this work, (○) [17], and (◇) [19].

The measured LO-phonon frequencies of  $AlGaSb$  are plotted as a function of Al composition in Figure 7. The composition dependence of the GaSb-like LO phonon frequencies determined from this study as well as those from previous works [17,19] are shown in Figure 6. The presented data are in good agreement with the reported data and were fitted to the quadratic expression:

$$v(cm^{-1}) = 234.3 - 10.67x + 24.28x^2 \quad (7)$$

### 4 Conclusions

$Al_xGa_{1-x}Sb$  epitaxial layers were grown at several Al contents by using the liquid phase epitaxy method at 400 °C on (001) GaSb substrates with x ranging between 0.05 and 0.2. The lattice parameters of the samples have been obtained from the mismatch components measured by HRXRD under the assumption that the epilayers' elastic deformation follows the first-order elasticity theory. From the comparison between the results obtained by the different experimental techniques, it has been possible to show that the lattice parameter of the layer increases nonlinearly with the Al content: Vegard's law is not obeyed. Raman scattering

measurements were used to measure the frequency shift and relative intensity of the optical GaSb like mode. The spectra show a clear splitting in frequency shift as the Al content varies. The TO and LO phonon frequencies of GaSb like mode shows a shift to low energies and their splitting decreases as the volume fraction of the corresponding binary constituent in the ternary layer decreases.

#### References:

- [1] P. S. Dutta, B. Méndez, J. Piqueras, E. Dieguez, H. L. Bhat, Nature of compensating luminescence centers in Te-diffused and -doped GaSb, *Journal of Applied Physics* 80 (1996) 1112-1115.
- [2] G. Milnes, A.Y. Polyakov, Gallium antimonide device related properties, *Solid-State Electronics* 36 (1993) 803-818.
- [3] M. F. Chioncel, C. Díaz-Guerra, J. Piqueras. Luminescence from indented Te-doped GaSb crystals, *Semiconductor Science and Technology* 19 (2004) 490-493.
- [4] P. S. Dutta, H. L. Baht, V. Kumar, The physics and technology of gallium antimonide: An emerging optoelectronic material. *Journal of Applied Physics* 81 (1997) 5821-5870.
- [5] A. T. Macrander, G. P. Schwartz, G. J. Gualtieri, X-ray and Raman characterization of AlSb/GaSb strained layer superlattices and quasiperiodic Fibonacci lattices, *Journal of Applied Physics* 64 (1988) 6733-6745.
- [6] S. G. Kim, H. Asahi, M. Seta, J. Takizawa, S. Emura, R. K. Soni, S. Gonda, H. Tanoue, Raman scattering study of the recovery process in Ga ion implanted GaSb. *Journal of Applied Physics* 74 (1993) 579-585.
- [7] C. E. M. Campos and P. S. Pizani, Strain effects on As and Sb segregates immersed in annealed GaAs and GaSb by Raman spectroscopy. *Journal of Applied Physics* 89 (2001) 3631-3633.
- [8] S. Winnerl, S. Sinning, T. Dekorsy, M. Helm, Increased terahertz emission from thermally treated GaSb. *Applied Physics Letters* 85 (2004) 3092-3094.
- [9] J. H. Dias da Silva, S. W. da Silva, and J. C. Galzerani, Crystallization process of amorphous GaSb films studied by Raman spectroscopy. *Journal of Applied Physics* 77 (1995) 4044-4048.
- [10] J. H. Dias da Silva, J. I. Cisneros, M. M. Guraya, G. Zampieri, Effect of deviation from stoichiometry and thermal annealing on amorphous gallium antimonide films. *Physical Review B* 51 (1995) 6272-6279.
- [11] F. M. Liu, T. M. Wang, L. D. Zhang, Raman properties of GaSb nanoparticles embedded in SiO<sub>2</sub> films. *Chinese Physics* 13 (2004) 2169-2173.
- [12] J. Olvera-Hernández, F. de Anda, H. Navarro-Contreras, V. A. Mishurnyi., "High purity GaSb grown by LPE in a sapphire boat". *Journal of Crystal Growth* 208 (2000) 27-32.
- [13] J. L. Lazzari, J. L. Leclercq, P. Grunberg, A. Joullié, B. Lambert, D. Barbusse and, R. Fourcade, Liquid phase epitaxial growth of AlGaAsSb on GaSb, *Journal of Crystal Growth* 123 (1992) 465-478.
- [14] D. I. Westwood, D. A. Woolf, Residual strain measurements in thick In<sub>x</sub>Ga<sub>1-x</sub>As layers grown on GaAs (100) by molecular beam epitaxy, *Journal of Applied Physics* 73 (1993) 1187-1192.
- [15] Landolt-Börnstein. Numerical data and functional relationships in science and technology. New Series. Group III: Crystal and Solid State Physics. Vol. 22: Semiconductors. Subvolume a: Intrinsic Properties of Group IV Elements and III-V, II-VI and I-VII Compounds. Ed. by O. Madelung Springer-Verlag Berlin-Heidelberg-New York-London-Paris-Tokyo 1987.
- [16] C. Bocchi, A. Bosacchi, C. Ferrari, S. Franchi, P. Franzosi, R. Magnanini, L. Nasi, Determination of lattice parameters in the epitaxial AlSb/GaSb system by high resolution X-ray diffraction, *Journal of Crystal Growth* 165 (1996) 8-14.
- [17] G. Lucovsky, K. Y. Cheng, G. L. Pearson, Study of the long-wavelength optic phonons in Ga<sub>1-x</sub>Al<sub>x</sub>Sb, *Physical Review B* 12 (1975) 4135-4141.
- [18] I. F. Chang, S. S. Mitra, Application of a Modified Random-Element-Isodisplacement Model to Long-Wavelength Optic Phonons of Mixed Crystals, *Physical Review* 172 (1968) 924-933.
- [19] R. Ferrini, M. Galli, G. Guizzetti, M. Patrini, A. Bosacchi, S. Franchi, R. Magnanini, Phonon response of Al<sub>x</sub>Ga<sub>1-x</sub>Sb/GaSb epitaxial layers by Fourier-transform infrared-reflectance and Raman spectroscopies, *Physical Review B* 56 (1997) 7549-7553.